SMAR 2017 – Fourth Conference on Smart Monitoring,
Assessment and Rehabilitation of Civil Structures

SMAR 2017

Torsional behavior of hollow-core FRP-concrete-steel bridge columns

Sujith Anumolu[1], Omar I. Abdelkarim[2], Mohanad M. Abdulazeez[3], Ahmed Gheni[3], and Mohamed A. ElGawady[4]

[1] Civil Engineer, Black & Veatch Corporation, Houston, USA
[2] Postdoctoral Fellow, Department of Civil Engineering, University of Sherbooke, Sherbrooke, Quebec, Canada
[3] Ph.D. candidate, Department of Civil, Architectural, and Environmental Engineering, Missouri University of Science and Technology, Rolla, MO, USA
[4] Benavides Associate Professor, Department of Civil, Architectural, and Environmental Engineering, Missouri University of Science and Technology, Rolla, MO, USA

ABSTRACT: This paper presents the behavior of hollow-core fiber reinforced polymer-concrete-steel (HC-FCS) column under pure torsion loading with constant axial load. The HC-FCS consists of outer FRP tube and inner steel tube with concrete shell sandwiched between the two tubes. The FRP tube was stopped at the surface of the footing and provided confinement to the concrete shell from outer direction. The steel tube was embedded into the footing to a length of 1.8 times to the diameter of the steel tube. The longitudinal and transversal reinforcements of the column were provided by the steel tube only. A large-scale HC-FCS column with a diameter of 610 mm and height of applied load of 2,438 mm with aspect ratio of 4 was investigated during this study. The study revealed that the torsional behavior of HC-FCS column mainly depended on the stiffness of the steel tube and the interactions among the column components (concrete shell, steel tube, and FRP tube).

1 INTRODUCTION

Columns of the curved and skewed bridges are undergoing axial, flexural, shear, and torsional loads during seismic excitations. Developing of new bridge systems had been focused by several researchers to reduce the seismic effects along with achieving construction acceleration. The accelerated bridge construction (ABC) had been developed in cost effective manner to decrease the on-site construction time and enhance work-zone safety. Concrete-filled steel tubes were developed as an ABC system in 1960s. This system significantly decreases the reinforcement detailing and workmanship for the construction. The presence of steel tube surrounding the concrete acts as permanent formwork, longitudinal and transverse reinforcement, and improves confinement to concrete core. While the concrete core acts as a bracing to the steel tube and provides lateral stability that delays local buckling in steel tube. The cost of construction of concrete-filled steel tubes is slightly higher than that of the reinforced concrete columns however it is lower than that of the steel columns. The fiber reinforced polymer (FRP) tube with high strength was used as an alternative to steel tube

introducing a system known as concrete-filled FRP tubular columns. Several researchers had investigated the concrete-filled FRP tubular columns under different loadings (Fam et al. 2003; ElGawady et al. 2010; Abdelkarim and ElGawady 2015). The corrosion resistance and confinement to the concrete core were improved by using fiber in place of steel. These studies revealed that the concrete-filled FRP exhibited high strength and ductility.

Teng et al. (2005) developed a new system known as hollow-core FRP-concrete-steel columns (HC-FCS) by exploiting the advantages of using three materials of FRP, concrete, and steel in addition to hollowing the column. This system consists of an outer FRP tube, an inner steel tube, and a concrete shell between them. Several researchers investigated the HC-FCS columns under different loadings including axial, flexural, combined axial and flexural, and impact loadings (Abdelkarim and ElGawady 2014; Ozbakkaloglu and Idris 2014; Abdelkarim and ElGawady 2016a and 2016b; Abdelkarim et al. 2016). The HC-FCS columns showed remarkable performances, high ductility, and high energy dissipation under these different loadings. However, according to the writers' best knowledge, no previous studies have been conducted on the HC-FCS columns under torsion loading. For the conventional reinforced concrete columns, it was observed that they had a moderate performance under torsion loading and the locking and unlocking of spiral reinforcement had significant effects on their behavior (Otsuka et al. 2004; Prakash et al. 2010). However, the hollow-core steel-concrete-steel column which consists of two concentric steel tubes with sandwiched concrete shell between them exhibited a remarkable performance in terms of strength and ductility under pure torsion loading (Anumolu et al. 2016). These results confirm the importance of investigating the torsional performance of the HC-FCS columns. Therefore, the current study presents the behavior of a large-scale HC-FCS column under pure torsion loading.

2 EXPERIMENTAL PROGRAM

2.1 Test specimens

A large-scale HC-FCS column was constructed and tested under constant axial load and cyclic torsional loading. The column dimensions and cross-sectional details were shown in figure 1. The column's height from the top of footing level was 2,032 mm and the torsional loading was applied at a height of 2,438 mm from the top of the footing level representing an aspect ratio of 4. The outer diameter of the FRP tube (D) and the inner steel tube (d) of the column was 610 mm and 356 mm, respectively. The thickness of the FRP tube (t_o) was 11 mm. The thickness of the steel tube (t_i) was 6.35 mm representing diameter-to-thickness (d/t_i) ratio of 56. The embedded length of the steel tube into the footing was 635 mm representing 1.8 times the diameter of the steel tube. The FRP tube was only between the surfaces of the footing and the loading head.

The dimension of the footing was 1,524 mm in length, 1,219 mm in width, and 863 mm in depth. A total of 6#7 steel rebars as top reinforcement, 7#7 steel rebars as bottom reinforcement, and 20#4 steel rebars as shear reinforcement were used for the footing. The dimension of the loading head was 762 mm in length, 762 mm in width, and 863 mm in depth. A clear cover of 25.4 mm spacing was maintained on all sides of the footing and the loading head.

2.2 *Material properties*

The FRP tube was manufactured by filament winding process and made of glass fibers and epoxy resin. The fiber orientation was ± 55° to the hoop direction of the tube. According to the manufacturer's data sheet, the axial compressive elastic modulus, axial ultimate stress, hoop elastic modulus, and hoop rupture stress of the FRP tube were 4.6 GPa, 83.7 MPa, 20.8 GPa, and 276.8 MPa, respectively. The elastic modulus, the yield stress, the ultimate stress, and the ultimate strain of the steel tube according to the manufacturer's data sheet were 200.0 GPa, 290.0 MPa, 400.0 MPa, and 0.23, respectively.

The concrete mixture was designed based on the required strength. The coarse aggregate used for concrete shell was pea gravel with maximum aggregate size of 9 mm. The water-cement (w/c) ratio was maintained at 0.5 for all the concrete members. The workability of the concrete shell was increased by the usage of High Range Water Reducers (HRWR). The concrete cylinders of the concrete shell and the footing were tested at 28 days and the day of test to measure the unconfined compressive strength. The column's concrete strengths at 28 days and day of test were 65.5 MPa and 66.9 MPa, respectively.

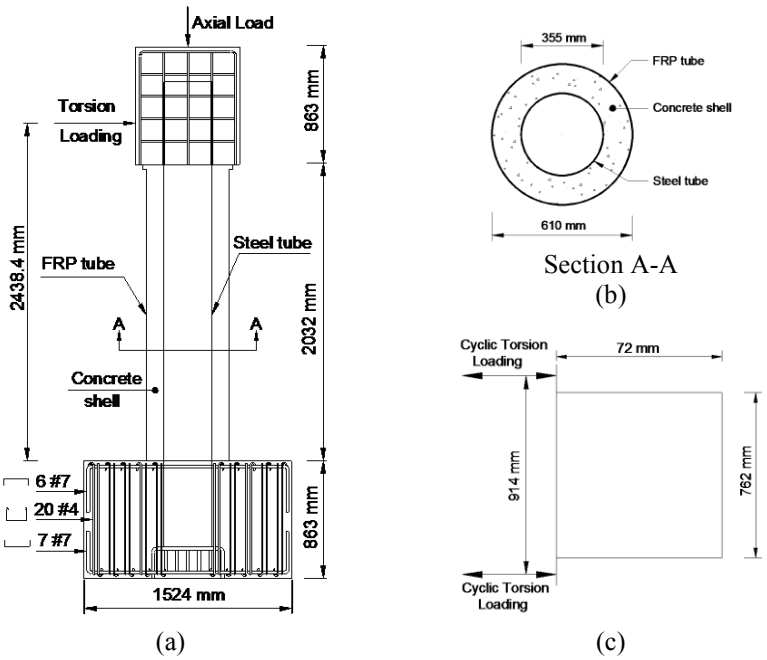

Figure 1. HC-FCS column (a) Elevation, (b) Cross-section, and (c) Plan of loading head

3 TEST SETUP AND INSTRUMENTATIONS

3.1 *General measurements*

Two servo-controlled hydraulic horizontal actuators from north direction were used to apply cyclic torsional load (figure 2). The axial load was applied on the loading head through hydraulic jacks (figure 2). Two load cells were placed between the loading head and hydraulic

jacks to monitor the applied axial load. The axial load was transferred from hydraulic jack to the column through six unbonded high strength pre-stressed tendons. The schematic test setup was shown in figure 2.

Strain gauges and rosettes, LVDTs' and string potentiometers were used to measure FRP and steel strains, column's deflection and deformations, respectively. The detailed instrumentations of the column was shown in figure 3. Total of 6 string potentiometers were attached at different locations along the column height (figure 3a). LVDTs were used to measure rocking, sliding of footing and slip of FRP tube over the loading head (figure 3a). Total of 48 strain gauges were attached on the FRP tube at six levels with spacing of 127 mm started from the top level of footing to 635 mm along the height of the column. At each level, total of 8 strain gauges (4 on hoop direction and 4 on vertical direction) were attached on east, west, north, and south directions (figure 3b). Total of 56 strain gauges were attached on the steel tube at seven levels with spacing of 127 mm started at 381 mm from bottom of the steel tube to 635 mm from bottom of the steel tube along the height of the column. At each level, total of 8 strain gauges with 4 on hoop direction and 4 on vertical direction were attached on east, west, north and south directions (figure 3b). Two Strain rosettes were attached on the steel tube at the surface level of the footing and 127 mm above it on north direction. Each strain rosette measures shear strain along with longitudinal strain and hoop strain. The buckling behavior of steel tube and slip of steel tube over concrete were monitored using cameras fixed inside the steel tube. Total of three cameras were fixed inside the steel tube along with light bulbs to provide illumination. The cameras were positioned at the top and bottom of the steel tube and at the surface level of the footing. String potentiometers were used to measure the twist angle of the column.

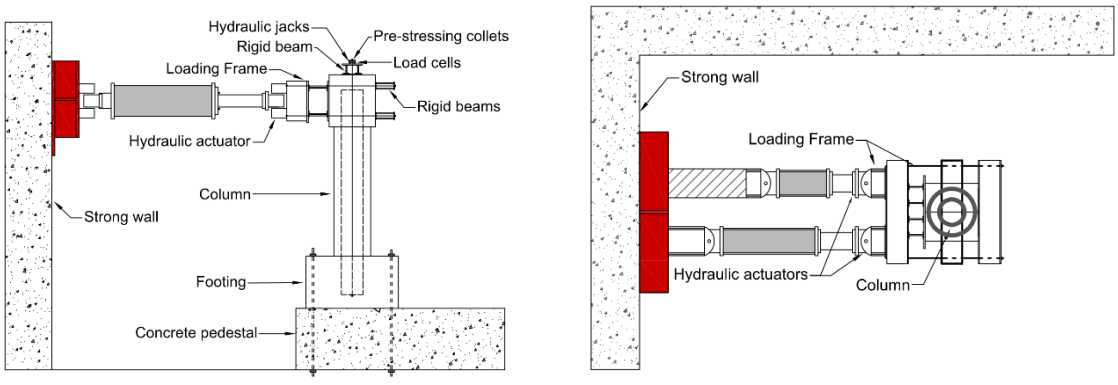

(a) (b)

Figure 2. Experimental Test Setup (a) Elevation, (b) Top view

3.2 Measuring of the column twist angle

The column's twist angle was defined as the angle of rotation of the column's head around its center. From the figures 3a and 3c, the distance between the two actuators on the loading head "a" was 914 mm. The column was rotated to a twist angle of 'θ' and the respective displacements 'Δ_1' and 'Δ_2' were determined from the actuators readings. Hence, the column's twist angle was determined using equation (1). Also, the rotation of the FRP tube was monitored in order to measure any slip occurred between the FRP tube and the column's head during the

application of the torsional loading. A string of length 'L' from the string potentiometer was attached to the top of the FRP tube of the column (figures 3a and 3d). The twist angle of the FRP "θ_1" determined using equations (2) and (3). The relative twist angle between the column's head and FRP tube was determined by subtracting "θ_1" from "θ". Another method was used to measure the relative the relative displacement between the FRP tube and the column's head. A wooden plate was attached to the top of the FRP tube parallel to the loading frame. Two LVDTs were attached horizontally to the loading frame and connected to the wooden plate to measure the respective displacements. Hence, the relative displacement was determined as similar to equation (1). Finally, the two methods to determine the relative displacement between the column's head and the FRP tube had very close results.

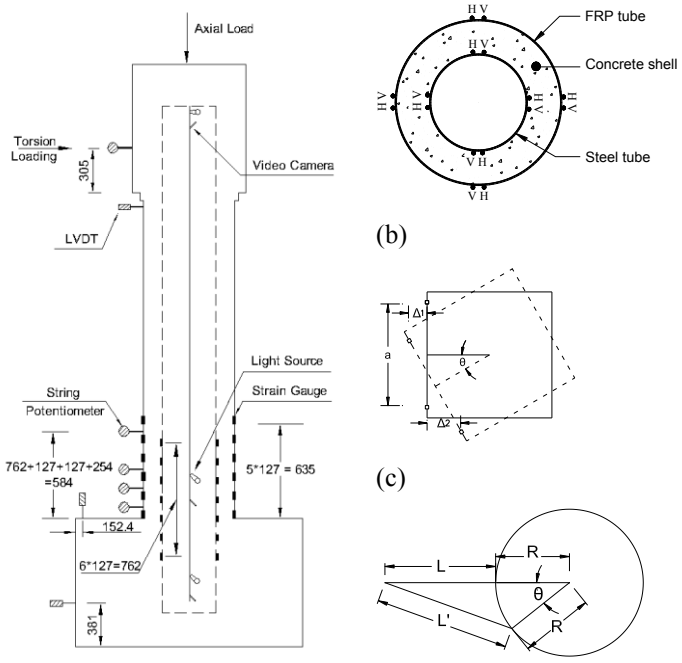

Note: All dimensions are in mm; H- horizontal Strain Gauge; V- vertical strain gauge

Figure 3. Test instrumentations: (a) General overview, (b) Strain gauges in cross-section, (c) Plan of measuring column's twist angle, and (d) Plan of measuring FRP twist angle

$$\text{The twist angle of the column, } \theta = Tan^{-1}\left(\frac{\Delta 1+\Delta 2}{a}\right) \quad (1)$$

$$Cos\ \theta_1 = \frac{(L+R)^2+R^2-L'^2}{2*L*R} \quad (2)$$

$$\text{From Eq. 2, } \theta_1 = Cos^{-1}\left(\frac{(L+R)^2+R^2-L'^2}{2*L*R}\right) \quad (3)$$

3.3 Loading Protocol

The axial load of 245 kN was applied on each hydraulic jack with a total axial force of 490 kN which represents 5% of the axial capacity of the reinforced concrete column with same outer diameter and 1% longitudinal reinforcement. The axial load was maintained constant throughout

the test and was monitored by load cells. The axial load capacity of reinforced concrete (P_o) was calculated from equation (4).

$$P_o = 0.85\, f_c'(A_c - A_s) + A_{st} f_y \quad (4)$$

Where, A_c and A_{st} are area of concrete and longitudinal steel reinforcement, respectively.

The cyclic torsional loading was applied through two servo-controlled hydraulic horizontal actuators from north direction. Displacement control technique was adopted to apply the torsional load on the column. The displacements of the two actuators were maintained at equal and opposite direction. The loading regime of the actuators was based on the FEMA (2007) recommendations in which the displacement amplitude of the each actuator was 1.4 times the previous displacement. Each of the displacement amplitude comprises of two cycles and frequency of each displacement cycle was set to 50 Hz. The displacement rate of the each actuator was varied between 0.25 mm/sec and 1.00 mm/sec. The loading regime used for cyclic torsional loading was shown in figure 4.

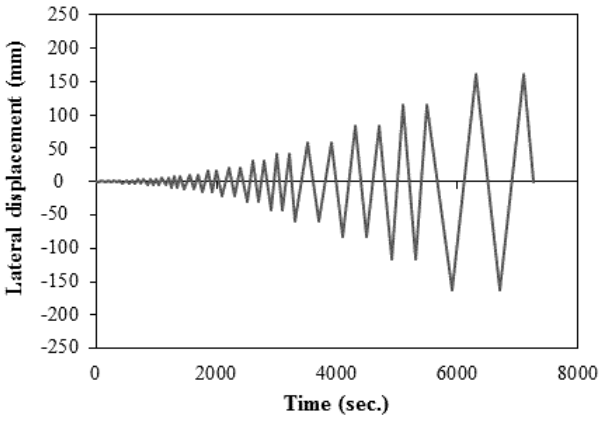

Figure 4. Loading regime for cyclic torsional loading

4 RESULTS AND DISCUSSION

The torque-twist angle hysteretic curve of the investigated HC-FCS column was shown in figure 5. The torque of the column was calculated by the summation of forces obtained from each actuator through load cells multiplied by half the distance between the actuators which was 457 mm. The actual twist angle of the column was obtained by subtracting the sliding effects of the footing during the test from the twist angle of the column that was determined by equation (1). The hysteretic curve started to be abnormal deviation in the column's torque after a twist angle of 7° due to additional force provided from the actuator because of the rotational constrain of the steel loading frame at high rotations. The experiment was stopped at a twist angle of 13.3° due to rotational limit in the arm of the actuator. The column reached torque of 173.5 kN.m in positive cycle and 185 kN-m in negative cycle at 7° twist angle in the column. The enhanced backbone curve was presented as dashed lines on the hysteretic curve as shown in figure 5a. The backbone curve was idealized the behavior of the column after removing the additional force provided from the actuator. From the enhanced backbone curve in figure 5a, the ultimate torque carried by the column was extended to 198 kN-m at a twist angle of 13.3°.

The column gained early stiffness and reached 70% of the column's ultimate torque at ±0.5° twist angle. The cohesion loss between the loading head and concrete shell occurred at ± 0.5° twist angle as shown in figure 5b. This behavior resulted in a slight degradation in the torque-twist angle curve however the drop was insignificant. After the loss of cohesion, the torque carried by the column was mainly depended on the stiffness of the steel tube and frictional force exerted between the concrete elements (footing, concrete shell, and loading head) and steel tube. The torque of the column continued to increase at low phase after the loss of cohesion due to the stiffness of the steel tube and existed frictional force between steel tube and concrete shell. Since there was no firm fixation of FRP tube in axial direction, the contribution of FRP tube towards torsional resistance was negligible. The presence of confinement and rigidity of FRP tube itself allowed the rotation of FRP tube along with the concrete shell.

The drop in the hysteretic curve at 3.5° column's twist angle in negative cycle was due to sudden sliding of steel tube over the concrete (figure 5b). The sudden sliding was noticed by the strain gauge readings and the cameras fixed inside the steel tube at negative 3.5° twist angle. However, the damage inside the concrete shell provided good friction and further prevents the sliding of steel tube at higher displacement cycles. Therefore, the torque continued to increase due to gaining in frictional force between the steel tube and the concrete. At higher load levels, the column's torque mainly depended on the friction exerted between the concrete and the steel tube.

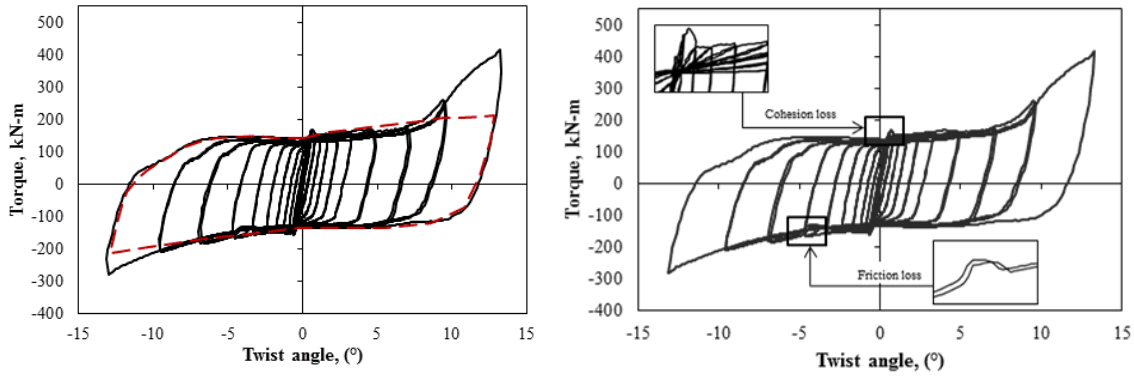

(a) (b)

Figure 5. Torque-twist angle of HC-FCS column under pure torsion: (a) hysteretic with backbone curves, (b) cohesion and friction less on the hysteretic curve

5 SUMMARY AND CONCLUSIONS

The torsional behavior of hollow-core FRP-concrete-steel (HC-FCS) column was investigated in the current study. The HC-FCS column consisted of concrete shell sandwiched between outer FRP tube and inner steel tube. The HC-FCS column had outer diameter of 610 mm and loading height of 2,438 mm with an aspect ratio of 4. The steel tube had an outer diameter of 356 mm. The FRP tube was placed on the surface of the footing while the steel tube was embedded into the footing to a length of 1.8 times the diameter of the steel tube. The HC-FCS column's longitudinal and transverse reinforcement was provided in the form of steel tube only. The following conclusions were revealed:

1. The torsional behavior of the HC-FCS column depended on the steel tube's stiffness and the friction existed between the steel tube and concrete.
2. The torsional strength of the HC-FCS column maintained even at larger rotations and exhibited good ductility.
3. The FRP tube contribution towards the torque was negligible and its confinement to the concrete core was minimal.

6 ACKNOWLEDGEMENT

This research was conducted at the Missouri University of Science and Technology, HighBay Laboratory. The kind contribution from ATLAS Tube is appreciated. Discount on the FRP tube from Grace Composites and FRP Bridge Drain Pipe is also appreciated. The authors also extend their appreciation to the National University Transportation Center (NUTC) at the Missouri University of Science and Technology for their contribution in support. However, any opinions, findings, and conclusions presented in this paper are those of the authors and do not necessarily reflect the views of the sponsors.

7 REFERENCES

Abdelkarim, O.I. and M.A. ElGawady, Concrete-Filled-Large Deformable FRP Tubular Columns under Axial Compressive Loading. Fibers, 2015. 3(4): p. 432-449.

Abdelkarim, O.I. and M.A. ElGawady, Analytical and Finite-Element Modeling of FRP-Concrete-Steel Double-Skin Tubular Columns. J. of Bridge Engineering, 2014.

Abdelkarim, O.I. and M.A. ElGawady, Performance of hollow-core FRP–concrete–steel bridge columns subjected to vehicle collision. Engineering Structures, 2016a. 123: p. 517-531.

Abdelkarim, O.I. and M.A. ElGawady, Behavior of hollow FRP–concrete–steel columns under static cyclic axial compressive loading. Engineering Structures, 2016b. 123: p. 77-88.

Abdelkarim, O.I., ElGawady, M.A., Gheni, A., Anumolu, S. and Abdulazeez, M., Seismic Performance of Innovative Hollow-Core FRP–Concrete–Steel Bridge Columns. Journal of Bridge Engineering, 2016, p.04016120.

Anumolu, S., O.I. Abdelkarim, and M.A. ElGawady, Behavior of Hollow-Core Steel-Concrete-Steel Columns Subjected to Torsion Loading. Journal of Bridge Engineering, 2016: p. 04016070.

ElGawady, M., A.J. Booker, and H.M. Dawood, Seismic behavior of posttensioned concrete-filled fiber tubes. J. of Composites for Construction, 2010. 14(5): p. 616-628.

Fam, A., B. Flisak, and S. Rizkalla, Experimental and analytical modeling of concrete-filled FRP tubes subjected to combined bending and axial loads. ACI Struct. J, 2003. 100(4): p. 499-509.

Federal Emergency Management Agency. Interim testing protocols for determining the seismic performance characteristics of structural and nonstructural components. Federal Emergency Management Agency (FEMA) 461, 2007, Washington, DC.

Otsuka, H., et al. Study on the seismic performance of reinforced concrete columns subjected to torsional moment, bending moment and axial force. in 13th World Conference on Earthquake Engineering. 2004.

Ozbakkaloglu, T. and Y. Idris, Seismic behavior of FRP-high-strength concrete–steel double-skin tubular columns. J. of Structural Engineering, 2014. 140(6): p. 04014019.

Prakash, S., A. Belarbi, and Y.-M. You, Seismic performance of circular RC columns subjected to axial force, bending, and torsion with low and moderate shear. Engineering Structures, 2010. 32(1): p. 46-59.

Teng, J. G., Yu, T., Wong, Y. L., and Dong, S. L. Innovative FRP-steel-concrete hybrid columns. Proc., 4th Int. Conf. on Advances in Steel Structures: ICASS 05, Z. Y.Shen, G. Q.Li, and S. L.Chan, eds., Elsevier, London, 2005, 545–554.